SUPPLEMENTARY INFORMATION

A new species of great ape from the late Miocene of Ethiopia

Gen Suwa[1], Reiko T. Kono[2], Shigehiro Katoh[3], Berhane Asfaw[4], and Yonas Beyene[5]

[1] *The University Museum, the University of Tokyo, Hongo, Bunkyo-ku, Tokyo, 113-0033 Japan*

[2] *Department of Anthropology, National Museum of Nature and Science, Hyakunincho, Shinjuku-ku, Tokyo, 169-0073 Japan*

[3] *Division of Earth Sciences, Hyogo Museum of Nature and Human Activities, Sanda, Hyogo, 669-1546 Japan*

[4] *Rift Valley Research Service, P.O. 5717, Addis Ababa, Ethiopia.*

[5] *Department of Archaeology and Paleontology, Authority for Research and Conservation of Cultural Heritage, Ministry of Culture and Tourism, P.O. Box 13247, Addis Ababa, Ethiopia*

1. Stratigraphic Provenience

The detailed stratigraphy of the Beticha locality (N8°52' E40°18') and its lithostratigraphic correlation with the "type site" (N8°53.5' E40°18.5') are given in Supplementary Figure 1. Both localities represent tilted fault blocks striking NE with steep NW dips, in some places exceeding 40 degrees. At both localities the entire sedimentary sequence is underlain by a conspicuous rhyolitic ignimbrite, previously dated to 10.7 ± 0.2 (20) or 11.0 ± 0.45 (17) by the K-Ar method. Lacustrine diatomites and/or diatomaceous silts dominate the sequence, with fluvial sandy to pebbly beds occurring at the lower and uppermost levels. The Beticha locality, situated approximately 3 km south of the type site towards the rift shoulders, exhibits more limited lacustrine facies. The type site sequence intercalates numerous thin silicic tuffs/bentonites, generally less than 30 cm thick. Two volcanic ash layers, from the lower and middle levels, respectively, can be correlated between the two localities based on their near-identical lithological and petrological characteristics (Supplementary Figure 2). Additionally, at both localities, a unique pumiceous tuff layer intercalates the uppermost sandy/pebble beds, providing further lithostratigraphic control. At the type site, the pumiceous tuff layer is unconformably overlain by resistant pyroclastic flow deposits dated by the K-Ar method to 10.10 ± 0.30 Ma (17). Thick rhyolitic ignimbrite/lavas just above these, or their equivalents at other sections, have been dated to 9.84 ± 0.30 (17), 10.5 ± 0.24 (20), and 9.3 ± 1.0 Ma (19, 21).

At the type site, fossiliferous sands occur below the major diatomaceous beds, which have been the focus of previous paleontological research (17, 18, 20). At the Beticha locality, fossils are scarce, with fragmentary and rarely identifiable fossils inconspicuously scattered on the surface. At these fossil occurrences, small patches of sediments around the pumiceous tuff layer are seen. All faunal remains, including the primate fossils, come from this surface scatter, which is well exposed for only about a 60 m by 30 m spatial extent. The Beticha locality exposures themselves extend more widely, up to ~300 meters, but mostly expose either the lower or uppermost sequences, which are so far unfossiliferous.

The surface scatter of fossils occurs as weathered fragments, which form a part of a thin (mostly <~10 cm) surface lag. This lag is accumulated on the modern land surface, formed on the tilted exposures of stratigraphic position from just below to several meters above the pumiceous tuff layer. We excavated two small trenches that stratigraphically span the strata above the pumiceous tuff layer. This stratigraphic interval comprises silty to sandy conglomerate beds, including paleosol horizons with

root casts and calcite concretions (Supplementary Figure 1). We interpret this sequence to represent a quasi-continuous deposition of sediments by a braided river system at a lake margin setting that accumulated towards the end of the Chorora paleobasin subsidence. The totality of the available evidence suggests that the fragmentary mammalian fossils probably existed in the form of rare inclusions of this stratigraphic interval, the sediments of which are now mostly eroded away. Today, fossils occur as a part of the lag veneer at and adjacent to the small remnant patches of these sediments.

2. Associated Fauna and Paleoenvironments

The taxonomic representation of mammalian fossils recovered was as follows:

Proboscidea
    cf. Elephantidae
Perissodactyla
    Rhinocerotidae
    Equidae
        "*Hipparion*"
Artiodactyla
    Hippopotamidae
        cf. *Kenyapotamus*
    Suidae
    Giraffidae
        cf. *Paleotragus*
    Bovidae
        small-sized species
Primates
    Cercopithecidae
    Hominoidea
        Chororapithecus abyssinicus
Carnivora gen. and sp. indet.

Systematic 100% surface collections were undertaken at the hominoid find spots. At the ape canine find spot, a systematic surface pick was done for an area of 30 m^2, but this did not produce any further identifiable pieces. At the ape molar find spot, the systematic surface pick resulted in additional finds. Therefore, the operation was extended to include the entire slope and adjacent areas totaling approximately 200 m^2. Excavation and sieving of the lag was conducted.

From this operation, a total of approximately 330 bone/tooth fragments were recovered. Pieces identifiable to family or superfamily levels were rare and confined to

dental fragments. For the purpose of analysis, we considered specimens to be "identifiable" when they were close to around 1/8 of a tooth or larger. Outside of the controlled pick/sieve area, only teeth that were intact close to half size or more were collected or recorded.

The resulting taxonomic frequencies are summarized in Supplementary Figure 3. Despite the small sample sizes, the sparse fauna at the Beticha locality appears to indicate primate dominance. Hippos, suids and giraffids are more common than the open-habitat preferring equids and bovids. This pattern is suggestive of a lake margin forested habitat with some open mosaic.

3. Specimen Information

CHO-BT 3

This is a left lower canine lacking the tips of both root apex and crown tip. It was discovered as a surface find during field survey on February 13, 2006, by field assistant Kampiro Kairante, two meters away from a cercopithecoid partial phalanx found on the same day. The canine exhibits a thick basal crown whose dimensions are given in the text Figure 1 legend. The slope of the preserved buccal crown face suggests a low robust, rather than a tall slender, canine crown. The mesial shoulder is placed high, estimated roughly at or above half crown height, but it does not form a well-angulated corner. Associated with the (inferred) high shoulder position, the mesial cervical line exhibits an unusually deep contour. Wear occurs distally and lingually, including a basal heel-like wear zone that formed from contact with the upper canine tip. This is a wear pattern commonly observed in the honing C/P3 complexes of both female and male ape canines.

The maximum basal diameter of this canine is broadly comparable to that of female *Gorilla* and male *Ouranopithecus* canines (Supplementary Figure 4). The deep mesial cervical line and inferred high shoulder placement suggest a female attribution. A high shoulder placement at half of crown height or higher is commonly seen in female canines of both modern and Miocene apes, but more rarely (e.g. *P. paniscus* and *Pongo*) or almost never (e.g. *Gorilla* and *P. troglodytes*) in male canines. These observations suggest that this canine belonged to a female. However, its non-projecting mesial shoulder and lack of enamel bulge at the cervical line are characteristics of male canines (31), and are uncommon in females. Thus, we are not able to assess the sex of this canine with certainty. It could either have belonged to a female or a small male

(Supplementary Figure 4).

CHO-BT 4

This is a right upper molar, most likely M2. It was found in two pieces; the lingual piece was discovered as a surface find by field assistant Woganu Amerga on March 21, 2007, approximately 30 meters east of the CHO-BT 3 canine find spot. The buccal piece was found in the same general area (within about 5 meters) during sieving of surface lag. Its crown dimensions are given in the text Figure 1 legend. The presence of four well-developed major cusps, the lack of distal crown abbreviation, attenuation, or morphological complexity suggest that this is either an M1 or M2. Its large size and tendency for paracone dominance over metacone indicate that it is probably an M2 rather than M1. The mesiodistal diameter of this molar exceeds the maximum value recorded for a modest sample (*n*=46) of *Gorilla gorilla gorilla*, and is larger than the male means of the larger-toothed subspecies, *G. g. beringei* and *G. g. graueri* (Supplementary Figure 5). Crown shape is elongate mesiodistally, with its shape index (mesiodistal length divided by buccolingual breadth) value corresponding to the upper-most range of *Gorilla* variation. The mesial protocone crest extends mesiobucally, with a strong mesial orientation. In both mesiodistal and buccolingual crown diameters, this M2 is noticeably larger than the known homologues of both *Samburupithecus* and *Ouranopithecus*. The shape index is similarly distinct, in contrast to the buccolingually broader upper molars of *Ouranopithecus*.

CHO-BT 5

This is an almost complete right upper M3 discovered during surface lag pick, at a location approximately 3 meters west of the CHO-BT 4 find spot. The M3 serial attribution is based on distal crown attenuation and morphological complexity. Its crown dimensions are given in the text Figure 1 legend. In both mesiodistal and buccolingual diameters, this M3 is large, at the uppermost range of *Gorilla* and *Ouranopithecus* variation (Supplementary Figure 5). As with CHO-BT 4, the mesial protocone crest extends mesiobucally with a strong mesial directional component. From size, wear, and preservation, it is possible that this tooth comes from the same individual as CHO-BT 4. If this was the case, relative molar size would be distinctly M2>M3, as commonly seen in gorilla subspecies but not in *Samburupithecus* or *Ouranopithecus*.

CHO-BT 6

This is approximately three quarters of a right upper M3, lacking much of the

metacone and distal crown regions. It was assembled from three small fragments. The first piece was discovered as a surface find on March 21, 2007, by Woganu Amerga, at a location approximately 1.5 meters from the CHO-BT 4 find spot. The other two fragments were recovered during systematic surface lag pick and sieving of the general area (within about 4 meters). The combination of an attenuated distal crown, small hypocone, and lack of a distolingually facing occlusal area suggest attribution to M3 rather than M2. Its crown dimensions are given in the text Figure 1 legend. This M3 is considerably smaller and slightly more worn than CHO-BT 5. Its mesiodistal diameter falls at the lowest range of *Gorilla* variation (Supplementary Figure 5).

CHO-BT 7

This is an almost complete left lower M3, discovered by Chiro zone antiquities officer Haddis Shewangizaw, on March 21, 2007, approximately 10 meters east of the CHO-BT 4 find spot. Its crown dimensions are given in the text Figure 1 legend. This is a large specimen, corresponding in size to the largest examples of *Gorilla* and *Ouranopithecus* lower M3 (Supplementary Figure 5). Its trigonid crest and the distal slope of the metaconid support an extensive zone of functional occlusion with mesiolingual upper M3. The mesial crown face is broken, but preservation is sufficient to reveal the presence of a mesial marginal ridge at a distinctly low level relative to its prominent trigonid crest. The hypoconulid and cusp 6 regions are small, in contrast to the well-developed distal crown of *Ouranopithecus* lower M3s.

CHO-BT 8

This is a left partial lower molar, most likely M1, lacking the metaconid region. It was found during surface lag pick at a location about 4 meters east of the CHO-BT 4 and BT 6 find spots. Its estimated crown dimensions are given in the text Figure 1 legend. It is similar in size with *Gorilla* and *Ouranopithecus* lower M1s (Supplementary Figure 5). It exhibits a high postentocristid that is continuous across the longitudinal groove, and a low distal marginal ridge. Despite crown loss and advanced surface enamel weathering, saliency of the trigonid crest can be inferred from the preserved EDJ.

CHO-BT 9

This is a left lower molar fragment consisting of almost the entire metaconid. It was found during surface lag pick, at a location within the area circumscribed by the CHO-BT 4, BT 5, and BT 6 find spots. This metaconid is slightly larger than that of the

CHO-BT 7 M3, and substantially larger than would be the case with the CHO-BT 8 M1. It is possible that this fragment represents a lower M2 of the same individual as CHO-BT 7 and BT 8. This molar fragment shares with CHO-BT 7 a high and prominent trigonid crest.

CHO-BT 10

This is a lower molar fragment comprising almost the entire hypoconid, the size of which is broadly comparable with that of the CHO-BT 7 M3. However, its occlusal morphology suggests that the two are not antimeres. Judging from the details of the preserved occlusal ridges, including those adjacent to the buccal grooves across from the hypoconid, this molar fragment probably comes from the right side and is an M2 rather than M3. It was found during surface lag sieve, in the same general area as the initial find spots of CHO-BT 4 and BT 6. It lacks any clear indication of occlusal wear, and could represent an individual other than CHO-BT 7, BT 8, or BT 9. Preservation state also differs from the other lower molars.

CHO-BT 11

This is a right upper partial M3. It is either a small M3 broken across the mesial paracone and protocone positions, or a distal portion of a larger molar (such as CHO-BT 5) broken at the mesial metacone and hypocone positions. It was found during surface lag sieve, in the same general area as the CHO-BT 8 lower M1. If the former identification is correct, this partial molar is much smaller in size than the other *Chororapithecus* molars. It would in fact be comparable in size and morphology to known late Miocene hominid examples of *Sahelanthropus*, *Ar. kadabba* and/or *Orrorin*. If so, CHO-BT 11 may represent a second taxon with hominid or ancestral affinities. However, its fragmentary status and lack of diagnostic morphological signals caution against further speculation at this rudimentary stage of knowledge.

Summary of identifications and sorting

The *Chororapithecus* fossil materials comprise four maxillary and five mandibular teeth. As outlined above, the maxillary teeth come from a minimum of three individuals, with the possibility that CHO-BT 4 and BT 5 (right upper M2 and M3) come from the same tooth row. Similarly, with the possibility that CHO-BT 7, BT 8, and BT 9 (left lower M1, possibly M2, and M3) come from the same individual, the mandibular teeth represent a minimum of one to three individuals. The hypoconid fragment (CHO-BT 10) lacks any wear zone development, and hence probably belonged to an individual

younger than CHO-BT 7, BT 8, and BT 9. Although the CHO-BT 3 lower canine is compatible with CHO-BT 7, BT 8, and BT 9 in wear, its find spot is somewhat at a distance and lacks spatial continuity with that of the molars, which were all in greater proximity to each other. We therefore consider it probable that the canine and lower molars come from different individuals. The size and wear of the suggested maxillary and mandibular molar rows are compatible with coming from the same individual. However, since the mandibular molar set comes from the left side and the maxillary set the right side, it is also probable that they come from different individuals. From the foregoing, our preferred interpretation is that a minimum of three and probably a total of six or more individuals are represented.

4. Comparative Remarks

Features other than those referred to in the text may also be shared similarities with gorillas. Although low cusped, the crista obliqua of the upper M2 is distinct and not interrupted by the longitudinal groove. In the lower M1 not only the trigonid crest but also the postentocristid is prominent. The buccal face of the upper molars include planar metacone and paracone faces that are angled to each other, forming a bi-planar depression centered at the buccal groove. This feature is well expressed in gorilla upper molars, but is also seen as a part of the variation of other ape species, such as in *Pan*.

The described morphology of *Samburupithecus* (29, 32) lacks any emphasis of shearing structures, but, on the contrary, includes coarser and thicker enamel ridges that tend to fill the occlusal basin. However, the mesiodistally elongate upper postcanine teeth and depressed median buccal crown faces of the upper molars are features of *Samburupithecus* that are shared with *Gorilla* and *Chororapithecus*. Such similarities may suggest either convergence or actual phylogenetic affinities. Further remains of both *Samburupithecus* and *Chororapithecus* are needed to assess such potential relationships.

Despite the general size similarity of the *Chororapithecus* dentition with that of the near-contemporary *Ouranopithecus*, the currently available materials suggest divergent masticatory adaptations of the two genera. Among all known Miocene hominoids, *Ouranopithecus* is uniquely derived in combining a large postcanine dental size with reduced C/P3 sectoriality and honing function (33–35). This is interpreted by some to indicate phylogenetic affinities with Pliocene *Australopithecus* (34, 36, 37). The latter hypothesis, however, is effectively falsified by *Ardipithecus* and the other late Miocene

hominids (which have smaller postcanine and larger relative canine sizes) (1–8).

There are other details of the *Ouranopithecus* dentition that are best interpreted as a part of its postcanine megadontia. These include the weak heteromorphy of the upper premolars, molars with a tendency for a comparatively strong size gradient from M1 through M3, lower third molars with developed distal talonid (hypoconulid and accessory cusps), moderately molarized lower dp3, and an enamel thickness comparable to that of Pliocene *Australopithecus* species (33–41). *Chororapithecus* in part shares the last feature, thick enamel (see below), but the lower M3 does not exhibit developed distal cusps, and there is no evidence for relatively large upper and lower M3 sizes. Finally, due to the uncertainty of sexual attribution (see below), the Chorora lower canine is difficult to interpret, but the inferred low and robust canine crown of *Chororapithecus* differs from that of *Ouranopithecus* (Supplementary Figure 4), which tends to be proportionately slender and taller (33, 35).

5. Divergence Dates

The relative splitting dates of *Pan*, *Gorilla*, *Pongo*, and old world monkeys (OWM), based on the comparatively extensive molecular studies (10–13, 42, 43), are summarized as follows. Setting the *Gorilla* split equal to 1.0, the respective splitting point ranges are approximately as follows: *Pan* 0.65–0.85, *Pongo* 1.4–1.9, and OWM 2.8–3.6. If rate is constant, a *Gorilla* split of 10.5–12 Ma yields the following *Pan–Homo, Pongo*–African ape/hominid, and OWM–hominoid split ranges: *Pan* 7–10 Ma, *Pongo* 15–23 Ma, and OWM 29–43 Ma. The mid-range points combined with a *Gorilla* split of 12 Ma give splits of *Pan* 9 Ma, *Pongo* 20 Ma, and OWM 38 Ma.

The above summarized molecular predictions are in concert with the notion that the *Pongo* lineage existed in Africa prior hominoid migration to the Eurasian continent, the earliest such opportunity for dispersal (barring significant rafting) being at circa 17 Ma (44). If in fact the *Gorilla* split was 12 Ma, then the OWM split estimate (33.6–43 Ma) largely predates the earliest known definitive occurrence of catarrhines (*Propliopithecus* and *Aegyptopithecus*) (45), and many would consider this to be somewhat outside an acceptable boundary condition. However, it may be indicative of variable molecular rates of evolution across lineages (46, 47), with higher mutation rates in the OWMs (48) (and early hominoids) because of their shorter generation lengths (48, 49) and/or higher metabolic rate in relation to smaller body mass (50).

6. Micro CT Methods and Evaluation of Enamel Thickness

Scanning methods

Micro-computed tomography (micro-CT) of the comparative materials was undertaken by use of the TX225-Actis system (Tesco, Tokyo) at the University Museum, the University of Tokyo. Serial scans of entire tooth crowns were taken at isotropic voxel resolution of 28–46 microns depending on size of the molar, resulting in approximately 250–300 slices per molar, usually taken parallel to the occlusal plane. Fossil teeth were scanned at 130 kvp, 0.2–0.24 mA, with a copper pre-filter of 0.2 or 0.5 mm to minimize beam hardening artifacts. Each scan was reconstructed in 512×512 matrix from 720 or 900 views.

Visualization and segmentation

Visualization of the outer enamel surface (OES) was done by means of the half-maximum-height method, using softwares Analyze 6.0 (Mayo Clinic, MA), Amira 4.0 (Mercury Computer Systems, MA), and the Rugle series (CT-Rugle and Vol-Rugle) (Medic Engineering Inc., Kyoto). When necessary, surface polygon data were extracted by application of the marching cube algorithm, and exported into software Rapidform 2006 (Inus Technology, Seoul).

Segmentation for visualization of the enamel dentine junction (EDJ) was done as in reference (28) using the Rugle series and Amira. In the case of fossil specimens that showed weak CT value contrast between enamel and dentine, EDJ placement was determined qualitatively, at pixel resolution, by scrolling through successive reformatted slices in three orthogonal directions. With the key fossil specimens and subsets of the comparative modern samples, positive three-dimensional EDJ surface models were made. These were done at three times natural size, using the EDEN rapid prototyping system (Fasotec, Tokyo) at the National Museum of Nature and Science, Tokyo. The three-dimensional models were essential in the final determination of the fossil EDJ surfaces, and in gaining key morphological insights during the course of the comparative analysis.

EDJ and enamel thickness measurements were done using the customized routines of the Rugle series as detailed in our previous studies (27, 28).

EDJ metrics

The comparative samples used in the EDJ metric analysis (n=43) were as follows. *G. gorilla*, n=10; *Po. pygmaeus*, n=7; *P. troglodytes*, n=13; *P. paniscus*, n=9; *Au. africanus*, n=4; and *Au. robustus*, n=5. All modern molars were extracted from the jaws to enable

close-up high-resolution micro-CT data collection. A mixed M1–M3 serial sample was used, although we did observe possible subtle trends differentiating M1s from the posterior molars. Confining the comparative analysis to just the M2 and M3 actually decreases overlap between *Gorilla* and *Pan*, further emphasizing the similarity between *Chororapithecus* and *Gorilla*.

MEX, mesial crown extension length

This is a measure devised to quantify the degree of crown extension mesial to the protocone. It is defined as the projected distance from the mesial-most point of the EDJ mesial marginal ridge to the protocone–paracone line. In actual mensuration, crown orientation was first standardized to maximize projected trigon area (28), or approximated to such an orientation (with some of the fossils). Next, a vertical plane running through the protocone and paracone tips was defined. Finally, the mesial-most point of the EDJ mesial marginal ridge was determined and its distance to the protocone–paracone plane was measured.

MCP, mesial crest length (protocone to protoconule)

This measure quantifies crest length from protocone tip to the mesial marginal ridge. It is defined as the three-dimensional point to point distance from the protocone to protoconule EDJ tips. In specimens that do not show a protoconule with distinct or discernible EDJ projection, the mesiolingual cingular ridge was followed occlusally, and the location where this would intersect the EDJ mesial marginal ridge was taken as the protoconule equivalent. Note that the lingual termination of the epicrista may or may not coincide with this.

PAPR, paracone–protocone distance

The three-dimensional point to point distance from the EDJ protocone to paracone tips.

Enamel thickness metrics

The comparative samples used in the volumetric analysis (n=57) were the mixed serial and upper/lower molars used in our previous studies (28), except for the *P. paniscus* molars which were newly added. With the small samples of apes, there were no clear differences between upper and lower molars. Sample sizes were as follows: *G. gorilla*, n=6; *Po. pygmaeus*, n=7; *P. troglodytes*, n=25; *P. paniscus*, n=12; *Au. africanus*, n=2; and *Au. robustus*, n=6.

The comparative samples used in the linear thickness analysis (*n*=79) were confined to upper molars. Data for the modern ape samples were all based on micro-CT, with the following sample sizes: *G. gorilla*, *n*=10; *Po. pygmaeus*, *n*=22; *P. troglodytes*, *n*=16; *P. paniscus*, *n*=11, with the *Pongo* sample including subfossil specimens from Sumatra. The "non-robust" hominid sample includes natural fracture data of *Au. anamensis* (*n*=5), *Au. afarensis* (*n*=1), and micro-CT data of *Au. africanus* (*n*=5), *Au.* cf. *garhi* (*n*=1), and cf. early *Homo* (*n*=1). The "robust" *Australopithecus* sample includes micro-CT data of *Au. robustus* (*n*=5) and *Au. aethiopicus* (*n*=1).

Although comparisons of enamel thickness of *Chororapithecus* with that of modern apes and Pliocene hominids form an important part of the present study, a comparable analysis of Miocene hominoids is not possible at present. For example, a metric account of enamel thickness is available for only a single molar each of the large-bodied genus *Ouranopithecus* (40, 41) and *Gigantopithecus* (51). Enamel thickness of these two molars appears thick at both "functional" and "non-functional" side cusps. But because of methodological differences, and because the two molars were from the lower jaw (as opposed to the measured upper molars of *Chororapithecus*), the data are not directly comparable. Enamel thickness of a single lower molar of *Proconsul major* (40) and an upper and lower molar each of *P. nyanzae* have also been reported (52). However, the single *P. major* molar is moderately worn, the upper molar of *P. nyanzae* appears to have been measured in a section different from the standard buccolingual molar section, and data comparable to those of the present study are not necessarily available. Because of these confounding factors, it is difficult to compare enamel thickness among these Miocene hominoids.

Maximum lateral enamel thickness

This is the maximum three-dimensional radial enamel thickness of the lateral crown face, measured from EDJ to OES, when possible at a location opposite the major cusp tips. Radial thickness of the lateral crown face was defined as the minimum thickness from a given point of the EDJ to the OES. Maximum radial thickness refers to the maximum of such measures (27, 28). With some of the fossil comparative samples, comparable measures were taken on naturally fractured near-radial sections, at or up to about half-way along the cusp margins from the cusp tips. When two measures were available on either side of the crown face (e.g. paracone and metacone buccally, or protocone and hypocone lingually), these were averaged to obtain representative thicknesses of each of the crown faces.

With the CT-derived data, the initial volume data set was rotated and reformatted into standardized orientation (as per above), or, when this was not possible, by determining the

tooth axis from examination of surface-rendered views. Next, the vertical section that passes through the cusp tip and that intersects both lateral crown EDJ and OES contours at an overall "radial" situation (i.e. an approximate 3-dimensional "radial" section) was visually determined (27). Finally, the initial volume was reformatted to this final orientation, and the enamel thickness measured by half-maximum-height thresholding, or by visual determination of closest pixel in the cases of low contrast enamel-dentine interfaces in some of the fossils.

AETMA, average enamel thickness in relation to maximum area

This measure of thickness is enamel volume divided by maximum horizontal area of the tooth crown (28). It represents the total amount of enamel available for wear, relative to approximate areas of occlusion available through time. Maximum horizontal area was defined as the maximum cross section area in standardized orientation (as defined above) that includes both enamel and dentine. In fossil specimens, as necessary, gaps were filled by visual approximation in order to obtain informative estimations.

Supplementary Figure 1

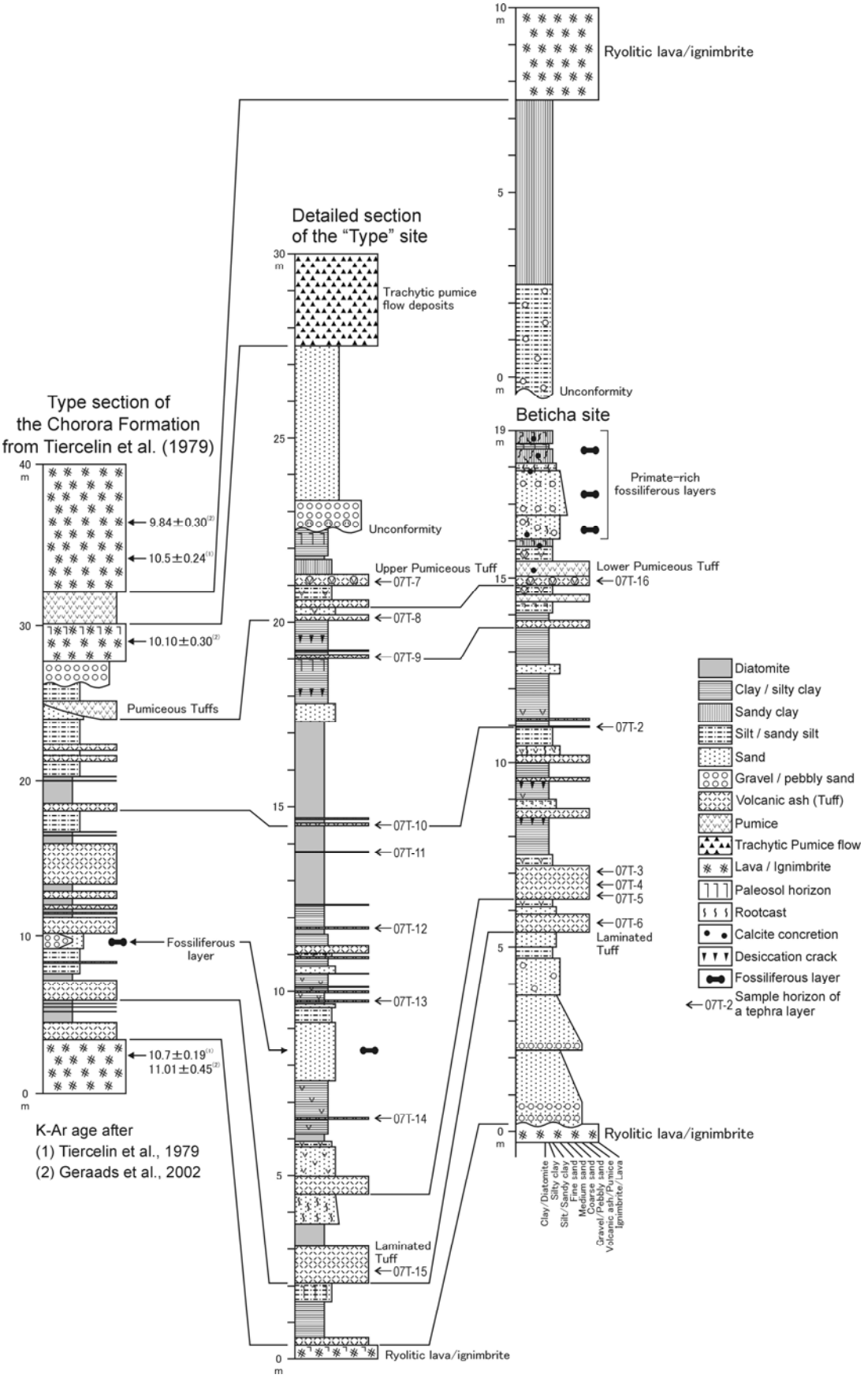

Lithostratigraphic correlation of the Beticha locality and type site.

Supplementary Figure 2

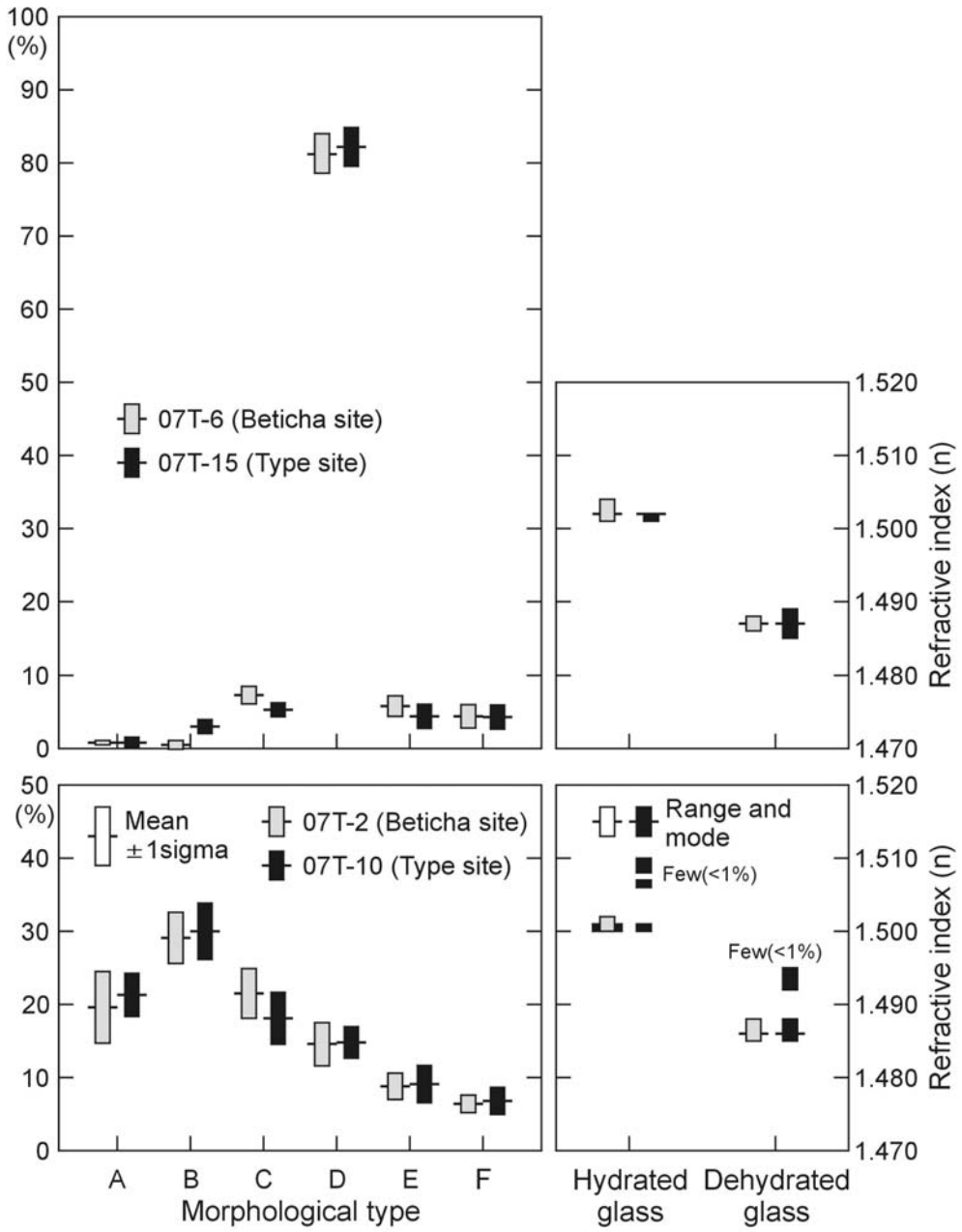

Tephrostratigraphic correlation based on glass shard morphology and the refractive index.

Note the tight similarity between two sets of correlative tephra: (1) 07T-6 and 07T-15, and (2) 07T-2 and 07T-10. The stratigraphic positions of these tephra are shown in Supplementary Figure 1. Shard morphology and refractive indices of hydrated and dehydrated glass shards are effective correlation tools for tephra under similar depositional, transportation, and preservation environments. Refractive indices of hydrated and dehydrated glass shards differ by about 0.015. This and the sharp modal peaks and narrow ranges indicate that the volcanic glass shards analyzed were fully hydrated with no effect of superhydration.

Supplementary Figure 3

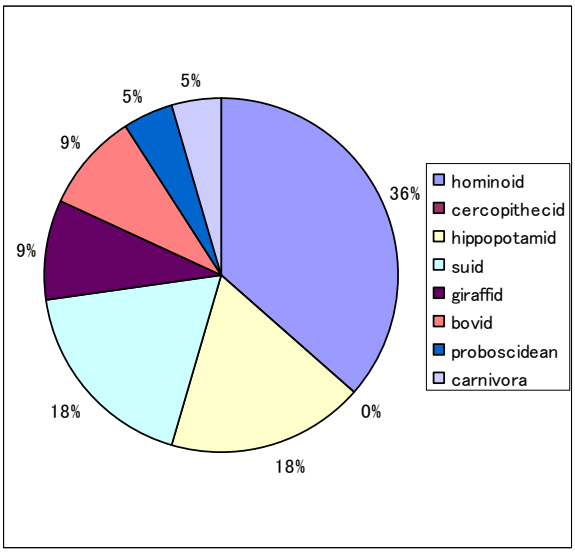

Relative abundance of the controlled surface pick/sieve assemblage from the ape molar site.

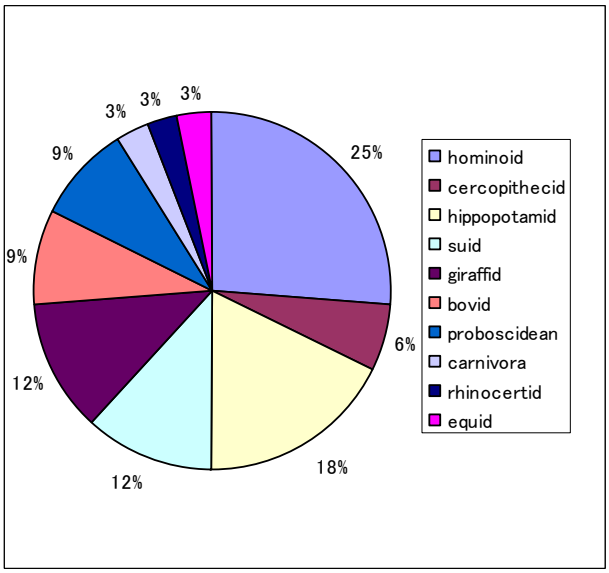

Relative abundance of all identifiable specimens from the Beticha locality.

Supplementary Figure 4

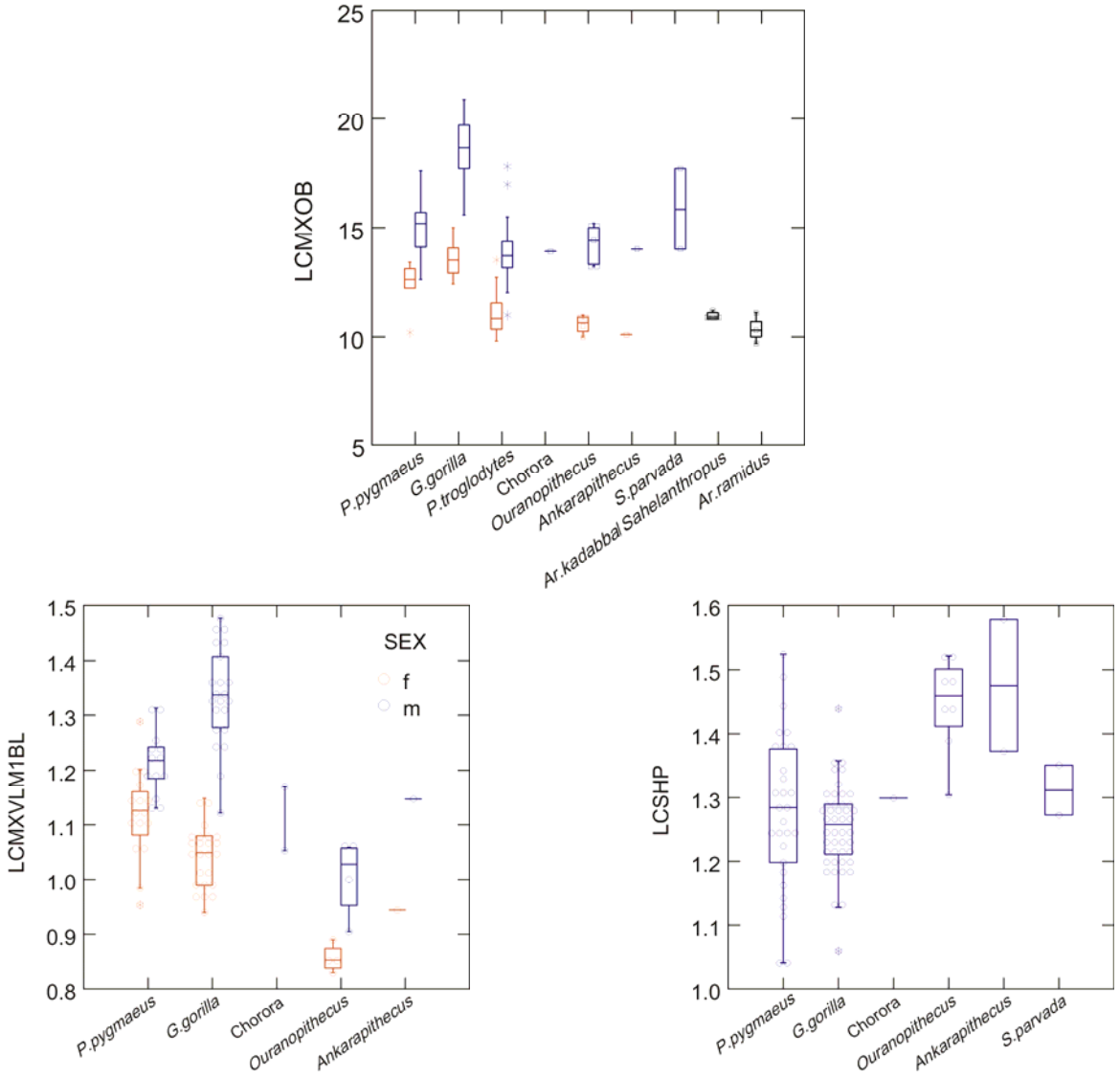

Lower canine comparative metrics.

Box plots of maximum diameter of lower canine (LCMAXOB), relative canine size (LCMXVLM1BL, maximum diameter divided by lower M1 buccolingual breadth), and canine basal crown shape (LCSHP, maximum diameter by perpendicular diameter). See Supplementary Figure 5 for information on comparative samples. Mesiodistal lengths and buccolingual breadths from the literature broadly correspond to the maximum and perpendicular diameters of the present study. Left (red) box plots female, right (blue) male, except in LCSHP (sex pooled). The isolated Chorora canine, which is difficult to sex, is comparable in size to female *Gorilla* and male *Pongo*, *Pan troglodytes*, *Ouranopithecus*, *Ankarapithecus*, and *Sivapithecus parvada* conditions. Because the Chorora canine is not associated with a molar, hypothetical relative sizes are plotted (LCMXVLM1BL). The lower data point is the Chorora canine divided by CHO-BT 8 buccolingual breadth, and the upper point by a hypothetical molar 10% smaller than CHO-BT 8. Note that either male or female attribution is possible for an ape with canine relative size ranging from *Ankarapithecus*, *Pongo* to *Gorilla* conditions.

Supplementary Figure 5

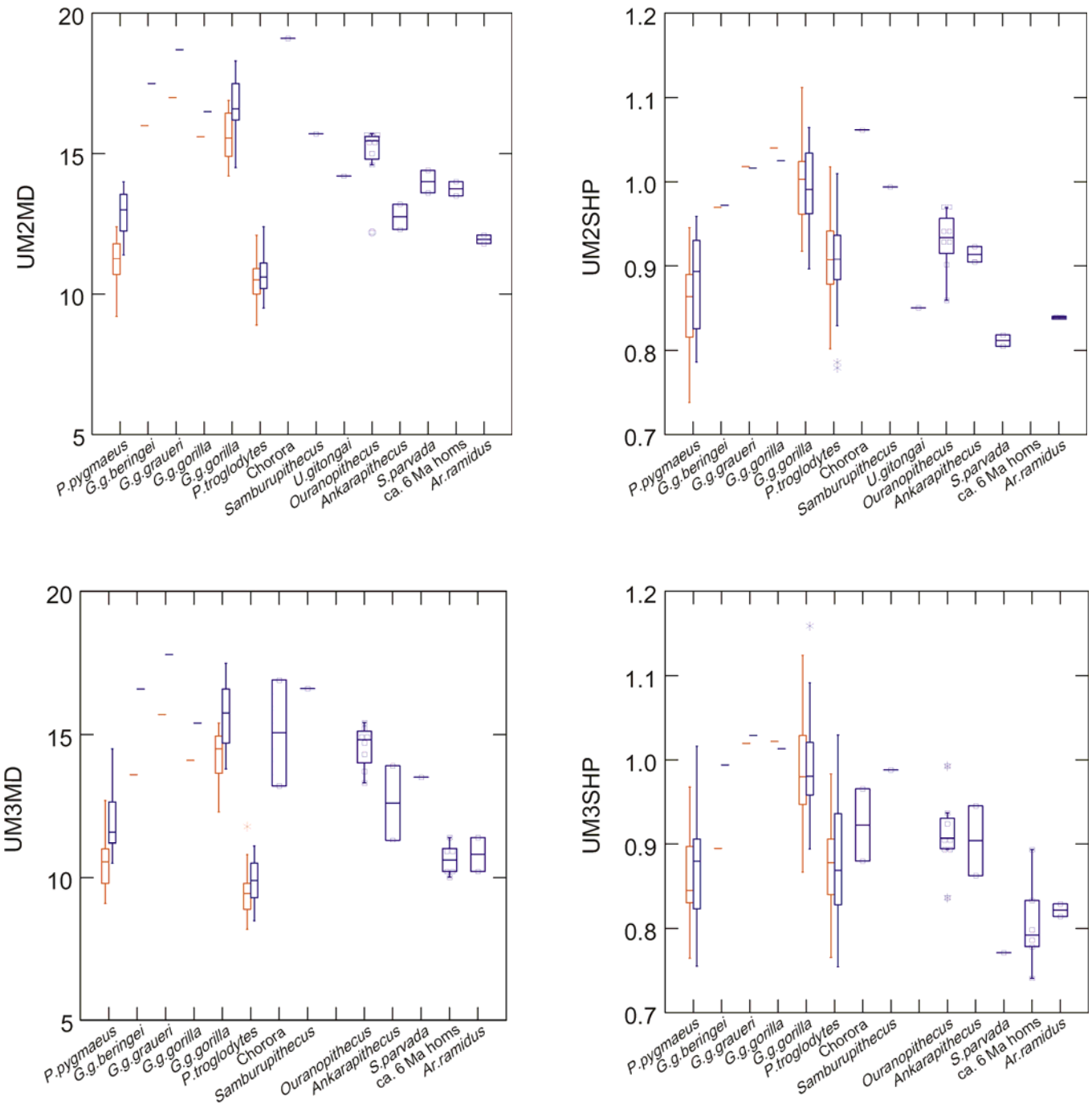

Upper M2 and M3 comparative crown metrics.

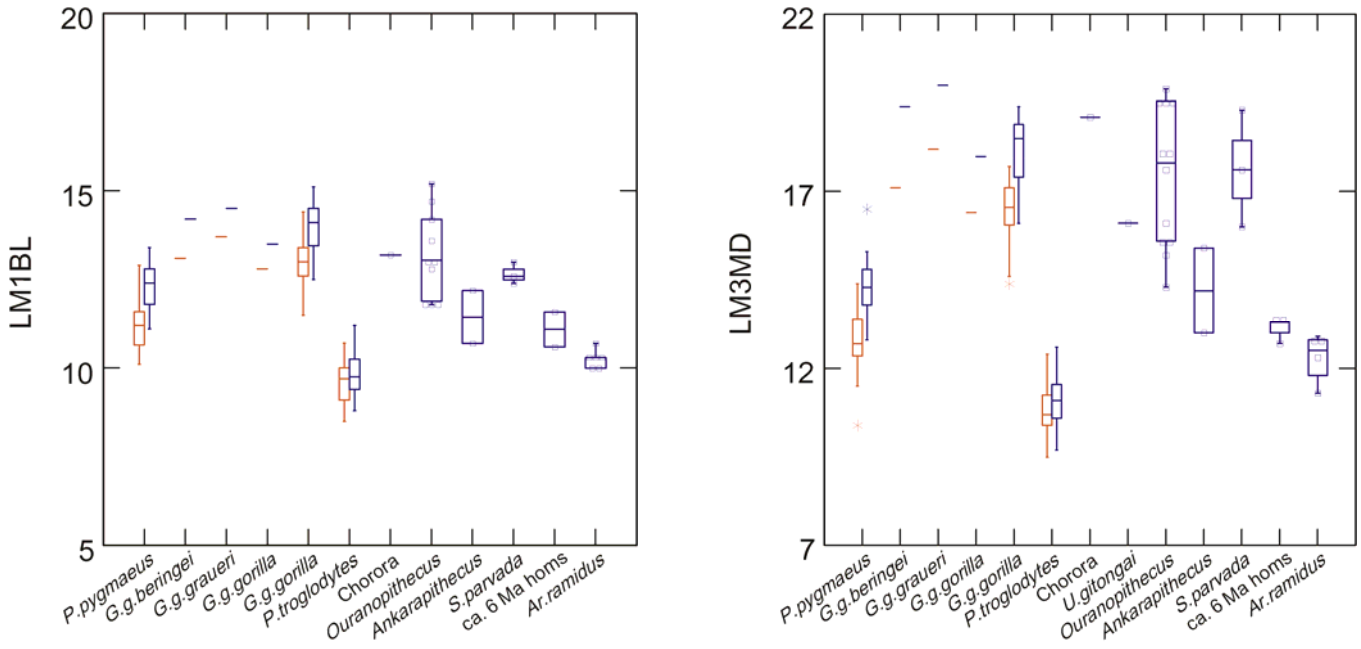

Lower M1 and M3 comparative metrics.

Box plots of upper and lower molar mesiodistal length (MD), buccolingual breadth (BL), and the shape index (SHP, mesiodistal length divided by buccolingual breadth). Modern samples are sex segregated, left (red) female, right (blue) male. Individual specimens are plotted for the fossils. Sample sizes for the modern species were as follows: *Pongo pygmaeus*, *n*= 30–38; *Pan troglodytes*, *n*=86–125; *Gorilla gorilla*, *n*=41–61. Gorilla subspecies plotted without ranges are the mean values taken from Uchida (53). Metrics of the fossil specimens were taken from the following references in parentheses: *Samburupithecus kiptalami* (29), "*Ugandapithecus*" *gitongai* (22), *Ouranopithecus macedoniensis* (33–36, 38, 39), *Ankarapithecus meteai* (54, 55), *Sivapithecus parvada* (56), *Ardipithecus ramidus* (1, 2), *Ar. kadabba* (3), *Orrorin tugenensis*, (5, 57), and *Sahelanthropus tchadensis* (6, 7). The ca. 6 Ma homs category combines the *Ar. kadabba*, *O. tugenensis*, and *S. tchadensis* materials available in the literature and the M3 from Lothagam upper Nawata member. Note that the measured Chorora molars range from the smallest to largest end of the *Gorilla* range of variation. Note also that the mesiodistally elongate crown shape of the Chorora upper M2 is matched only by *Gorilla* specimens.

8. Reference Notes

31) Kelley, J. Sexual dimorphism in canine shape among extant great apes. *Am. J. Phys. Anthropol.* **96**, 365–389 (1995).

32) Pickford, M. & Ishida, H. Interpretation of *Samburupithecus*, an Upper Miocene hominoid from Kenya. *C. R. Acad. Sci. (Paris)* **326**, 299–306 (1997).

33) Koufos, G. D. Mandible of *Ouranopithecus macedoniensis* (Hominidae, Primates) from a new late Miocene locality of Macedonia (Greece). *Am. J. Phys. Anthropol.* **91**, 225–234 (1993)

34) de Bonis, L & Koufos, G. D. The face and the mandible of *Ouranopithecus macedoniensis*: description of new specimens and comparisons. *J. Hum. Evol.* **24**, 469–491 (1993).

35) Koufos, G. D. & de Bonis, L. New material of *Ouranopithecus macedoniensis* from late Miocene of Macedonia (Greece) and study of its dental attrition. *Geobios* **39**, 223–243 (2006).

36) Koufos, G. D. & de Bonis, L. The deciduous lower dentition of Ouranopithecus macedoniensis (Primates, Hominoidea) from the late Miocene deposits of Macedonia, Greece. *J. Hum. Evol.* **46**, 699–718 (2004).

37) de Bonis, L. & Koufos, G. D. *Ouranopithecus* et la date de séparation des hominoïds modernes. *C. R. Palevol* **3**, 257–264 (2004).

38) Koufos, G. D. The first female maxilla of the hominoid *Ouranopithecus macedoniensis* from the late Miocene of Macedonia, Greece. *J. Hum. Evol.* **29**, 385–399 (1995).

39) de Bonis, L., Koufos, G. D., Guy, F., Peigné, S. & Sylvestrou, I. Nouveaux restes du primate hominoïde *Ouranopithecus* dans les dépôts du Miocène supérieur de Macédoine (Grèce). *C. R. Acad. Sci. (Paris)* **327**, 141–146 (1998).

40) Andrews, P. & Martin, L. Hominoid dietary evolution. *Phil. Trans. R. Soc. Lond. B* **334**, 199–209 (1991).

41) Smith, T. M., Martin, L. B., Reid, D. J., de Bonis, L. & Koufos, G. D. An examination of dental development in *Graecopithecus freybergi* (=*Ouranopithecus macedoniensis*). *J. Hum. Evol.* **46**, 551–577 (2004).

42) Sibley, C. G. & Ahlquist, J. E. DNA hybridization evidence of hominoid phylogeny: Results from an expanded data set. *J. Molec. Evol.* **26**, 99–121 (1987).

43) Caccone, A. & Powell, J. R. DNA divergence among hominoids. *Evolution* **43**, 925–942 (1989).

44) Heizmann, E. P. J. & Begun, D. R. The oldest Eurasian hominoid. *J. Hum. Evol.* **41**,

463–481 (2004).
45) Seiffert, E. R. Revised age estimates for the later paleogene mammal faunas of Egypt and Oman. *Proc. Natl. Acad. Sci.* **103**, 5000–5005 (2006).
46) Hasegawa, M., Thorne, J. L. & Kishino, H. Time scale of eutherian evolution estimated without assuming a constant rate of molecular evolution. *Genes Genet. Syst.* **78**, 267–283 (2003).
47) Elango, N., Thomas, J. W., NISC Comparative Sequencing Program, Yi, S. V. Variable molecular clocks in hominoids. *Proc. Natl. Acad. Sci.* **103**, 1370–1375 (2006).
48) Yi, S., Ellsworth, D. L. & Li, W.-H. Slow molecular clocks in old world monkeys, apes, and humans. *Mol. Biol. Evol.* **19**, 2191–2198 (2002).
49) Lovejoy, C. O., Burstein, A. H. & Heiple, K. G. Primate phylogeny and immunological distance. *Science* **176**, 803–805 (1973).
50) Gillooly, J. F., Allen, A. P., West, G. B. & Brown, J. H. The rate of DNA evolution: Effects of body size and temperature on the molecular clock. *Proc. Natl. Acad. Sci.* **102**, 140–145 (2005).
51) Dean, M. C. & Schrenk, F. Enamel thickness and development in a third permanent molar of *Gigantopithecus blacki. J. Hum. Evol.* **45**, 381–387 (2003).
52) Beynon, A. D., Dean, M. C., Leakey, M. G., Reid, D. J. & Walker, A. Comparative dental development and microstructure of *Proconsul* teeth from Rusinga Island. *J. Hum. Evol.* **35**, 163–209 (1998).
53) Uchida, A. *Craniodental Variation Among the Great Apes, Peabody Museum Bulletin 4* (Harvard Univ. Press, Cambridge, 1996).
54) Alpagut, B. *et al*. A new specimen of *Ankarapithecus meteai* from the Sinap Formation of central Anatolia. *Nature* **382**, 349–351 (1996).
55) Begun, D. R. & Güleç, E. Restoration of the type and palate of *Ankarapithecus meteai*: Taxonomic and phylogenetic implications. *Am. J. Phys. Anthropol.* **105**, 279–314 (1998).
56) Kelley, J. A new large species of *Sivapithecus* from the Siwaliks of Pakistan. *J. Hum. Evol.* **17**, 305–324 (1988).
57) Pickford, M. & Senut, B. Hominoid teeth with chimpanzee- and gorilla-like features from the Miocene of Kenya: implications for the chronology of ape-human divergence and biogeography of Miocene hominoids. Anthropol. Sci. 113, 95–102 (2005).